Journal of Materials Chemistry C

PAPER

View Article Online
View Journal | View Issue

Cite this: J. Mater. Chem. C, 2014, 2, 9398

A systematic identification of efficiency enrichment between thiazole and benzothiazole based yellow iridium(III) complexes†

Thota Giridhar,‡[a] Woosum Cho,‡[a] Young-Hoon Kim,‡[b] Tae-Hee Han,[b] Tae-Woo Lee*[b] and Sung-Ho Jin*[a]

Received 12th July 2014
Accepted 19th September 2014

DOI: 10.1039/c4tc01514b

www.rsc.org/MaterialsC

Four cyclometalated heteroleptic Ir(III) complexes [(Et-Cz-BTz)$_2$Ir(pic)], [(Et-Cz-BTz)$_2$Ir(pic-N-O)], [(Et-Cz-BTz)$_2$Ir(EO$_2$-pic)], and [(Et-Cz-BTz)$_2$Ir(EO$_2$-pic-N-O)] containing benzothiazole linked ethylcarbazole (Et-Cz-BTz) as a main ligand have been successfully synthesized for solution-processed phosphorescent organic light-emitting diodes (PhOLEDs). All the Ir(III) complexes emit bright yellow (541–582 nm) phosphorescence at room temperature. Among the four Ir(III) complexes, the [(Et-Cz-BTz)$_2$Ir(EO$_2$-pic)] showed the best luminous efficiency of 60 cd A^{-1} and external quantum efficiency (EQE) of 19% with CIE coordinates (0.467, 0.524), which is one of the best efficiencies for solution-processed yellow PhOLEDs using heteroleptic Ir(III) complexes as an emitting layer. Interestingly, upon replacing the thiazole linking group in the main ligand by benzothiazole, the EQE increased from 6.08 to 19%.

1. Introduction

Phosphorescent organic light-emitting diodes (PhOLEDs) based on heavy metal centred phosphorescent emitters are currently attracting a lot of attention due to their potential applications in full color flat panel displays and solid state lighting.[1–4] Particularly, these kind of emitters in the emitting layer (EML) can harvest both singlet and triplet electro-generated excitons, which leads to an increase in the internal quantum efficiency as high as the theoretical value of 100%.[5–8] Particularly, the emitters based on Ir(III) complexes have become the most successful phosphorescent candidates in recent days owing to their favourable electrochemical and photophysical properties, flexible color tunability, short triplet state lifetimes, and the ability to participate in outer sphere electron transfer reactions.[9–11] Even though various colors of phosphorescent Ir(III) complexes can be prepared by varying the structure of the ligands, the yellow emitting Ir(III) complexes have attracted more research interest because of their utility in the fabrication of two emitting component white OLEDs with blue emitters.[12]

When considering the efficiency point of view, the achieved maximum efficiencies of solution-processed yellow PhOLEDs are not as high as those of other primary color materials (blue, green, and red ~20%). Recently, Bryce *et al.* reported the systematic study of the substituent effects of Ir(III) complexes containing carbazole (Cz)-pyridine based main ligands for solution-processed OLEDs. These were fabricated using poly(*N*-vinylcarbazole) as a high triplet energy host material and as a hole transport material, and very high external quantum efficiencies (EQE), of the order of 12%,[10] was achieved. Further, we introduced ethylcarbazole-thiazole (Et-Cz-Tz) based main ligands in Ir(III) complexes and studied their efficiency in solution-processed PhOLEDs using *m*-MTDATA:TPBI as host material, and among the Ir(III) complexes, the most promising Ir(III) complex showed a maximum EQE of 6.08%.[13] Moreover, the introduction of a benzothiazole (BTz) based framework into the ligands of Ir(III) complexes leads to efficient yellow emission.[11] Even when various electron donating/withdrawing groups (OMe, Me, CF$_3$, F, CN, *etc.*) or more extended chromophores are introduced either in the phenyl ring or to the BTz moiety, the phosphorescence of the resultant Ir(III) complexes is mainly localized within a narrow color range around yellow with few exceptions.[14–16] Very recently, Li *et al.* reported Ir(III) complexes with Cz-BTz based ligand systems for vacuum-deposited PhOLEDs and observed an EQE of 23%.[12]

The PhOLEDs fabricated using thermal high vacuum deposition techniques show better device performance, solution process techniques, such as spin coating and inkjet printing, have more advantages than the former because of their less complicated fabrication process and limited utilization of

[a]Department of Chemistry Education, Graduate Department of Chemical Materials and Institute for Plastic Information and Energy Materials, Pusan National University, Busan, 609-735, Korea. E-mail: shjin@pusan.ac.kr; Fax: +82-51-581-2348; Tel: +82-51-510-2727

[b]Department of Materials Science and Engineering, Pohang University of Science and Technology (POSTECH), San 31 Hyoja-dong, Nam-gu, Pohang, Gyungbuk, 790-784 Korea

† Electronic supplementary information (ESI) available. See DOI: 10.1039/c4tc01514b

‡ These authors contributed equally to this work.

expensive materials.[17–19] Thus, much attention has been given in the area of solution-processed PhOLEDs for the design and preparation of suitable small molecules and the optimization of device architectures. In order to fabricate the solution-processed PhOLEDs, the Ir(III) complexes are prepared using oligomeric or polymeric ligand systems[20,21] or dendrimers.[22,23] Upon introduction of these macromolecular systems into the Ir(III) complexes, the purity of the resultant material decreases. Moreover, multi-step reaction sequences are required to obtain the macromolecular ligands. Thus, solution-processed counterparts, which combine the advantageous features of both polymeric and small molecule materials, have been developed. Given these circumstances, the development of solution process heavy metal centred phosphorescent emitters is of great importance.

In this report, in order to further validate the above discussions, we attached BTz to *N*-ethylcarbazole (Et-Cz-BTz) as a main ligand in Ir(III) complexes for solution-processed PhOLEDs, where the solubilizing ethoxyethanol group was introduced into the ancillary ligands by a tandem reaction approach.[13] Here, we synthesized four cyclometalated heteroleptic Ir(III) complexes using Et-Cz-BTz as a main ligand and picolinic acid [(Et-Cz-BTz)$_2$Ir(pic)], picolinic acid N-oxide [(Et-Cz-BTz)$_2$Ir(pic-N-O)], 4-(2-ethoxyethoxy)picolinic acid [(Et-Cz-BTz)$_2$Ir(EO$_2$-pic)], and 4-(2-ethoxyethoxy)picolinic acid N-oxide [(Et-Cz-BTz)$_2$Ir(EO$_2$-pic-N-O)] as ancillary ligands. All the Ir(III) complexes show bright yellow emission (541–582 nm) at room temperature. The photophysical and electrochemical properties of these Ir(III) complexes, as well as the performance of their solution-processed PhOLEDs, were investigated systematically.

2. Experimental

2.1. General information

All chemicals and reagents were purchased from Aldrich Chemical Co. and used without further purification. THF was purified by appropriate procedures and the other solvents were used as received. 3-Bromo-9-ethyl-9*H*-carbazole, 9-ethyl-3-(4,4,5,5-tetramethyl-1,3,2-dioxaborolan-2-yl)-9*H*-carbazole (1) and 4-chloropicolinic acid N-oxide were synthesized using our previously reported procedures. All reactions were systematically monitored by thin layer chromatography with Merck pre-coated aluminum plates. ^{1}H- and ^{13}C-NMR spectra were recorded on a Varian Mercury Plus 300 MHz spectrometer in $CDCl_3$ using tetramethylsilane as an internal standard. High resolution mass spectra were obtained from the Korea Basic Science Institute, Daegu Centre (HR-ESI Mass). TGA and DSC thermograms were obtained with Mettler Toledo TGA/SDTA 851e and DSC 822e analysers, respectively, under a N_2 atmosphere at a heating rate of 10 °C min^{-1}. The UV-visible absorption and fluorescence spectra were recorded with a JASCO V-570 UV-vis spectrophotometer and a Hitachi F-4500 fluorescence spectrophotometer, respectively, at room temperature. CV measurements were performed with a CHI 600C potentiostat (CH Instruments), which was equipped with a platinum disc as the working electrode, a platinum wire as the counter electrode, and a Ag/AgCl as the reference electrode, at a scan rate of 100 mV s^{-1} using anhydrous chloroform and 0.1 M tetrabutylammonium tetrafluoroborate ($TBABF_4$) as the solvent and electrolyte, respectively. The potentials were referenced to the ferrocene/ferrocenium redox couple (Fc/Fc^+). It was assumed that the redox potential of Fc/Fc^+ had an absolute energy level of −4.8 eV under vacuum. All electrochemical experiments were carried out at room temperature.

2.2. Synthesis of 2-(9-ethyl-9*H*-carbazol-3-yl)benzothiazole (Et-Cz-BTz) (2)

2-Bromobenzothiazole (6.66 g, 31.13 mmol), K_2CO_3 (12.89 g, 93.39 mmol), and tetrakis(triphenylphosphine)palladium (1.79 g, 1.56 mmol) were added to a solution of 9-ethyl-3-(4,4,5,5-tetramethyl-1,3,2-dioxaborolan-2-yl)-9*H*-carbazole (1) (10 g, 31.13 mmol) in 100 mL of THF under N_2 atmosphere. The reaction mixture was heated to 65 °C for 15 h. After completion of the reaction, the solution was cooled to room temperature, poured into water and extracted with EA. The organic layer was washed with water and brine solution, and then dried over anhydrous $MgSO_4$. The solvent was removed under reduced pressure and the crude product was purified by column chromatography on silica gel using EA/hexane (2 : 8 v/v) as an eluent to give 2-(9-ethyl-9*H*-carbazol-3-yl)benzothiazole (Et-Cz-BTz) (6.2 g, 62%) as a white solid. m.p. 142 °C. ^{1}H-NMR (300 MHz, $CDCl_3$): δ (ppm): 8.86 (s, 1H), 8.22–8.19 (dd, 2H), 8.09 (d, 1H), 7.92 (d, 1H), 7.55–7.28 (m, 6H), 4.44–4.37 (q, 2H), 1.48 (t, 3H). ^{13}C-NMR ($CDCl_3$): δ 169.6, 154.6, 141.8, 140.8, 135.2, 126.6, 126.4, 125.8, 124.9, 124.8, 123.7, 123.3, 122.9, 121.7, 121.1, 120.3, 119.9, 109.1, 108.9, 38.0, 14.1.

2.3. General procedure for the synthesis of Ir(III) complexes

All the Ir(III) complexes were synthesized by applying a general procedure reported by our group.[13,24–26] The general procedure for the synthesis of Ir(III) complexes is as follows: compound 2 (6 g, 18.26 mmol) and $IrCl_3 \cdot 3H_2O$ (2.18 g, 7.31 mmol) were added to a mixture of 2-ethoxyethanol and water (80 mL, 3 : 1 v/v). The resultant mixture was refluxed at 140 °C for 20 h under an N_2 atmosphere and cooled to room temperature. The formed yellow solid was filtered and washed with water, followed by methanol. Subsequently, the solid was dried in a vacuum oven at 120 °C to afford cyclometalated Ir(III) μ-chloride bridged dimer (3) as a yellow solid (4.8 g, 60%). A solution of 3 (1 g, 0.57 mmol), 5 equivalents of ancillary ligand and Na_2CO_3 (0.60 g, 5.7 mmol) in 2-ethoxyethanol (20 mL) was refluxed under N_2 for 12 h. After cooling to room temperature, the mixture was poured into water and extracted with MC. The organic layer was dried over anhydrous $MgSO_4$, filtered, and the solvent was removed under reduced pressure. The crude product was purified by silica gel column chromatography using EA : MC : hexane (2 : 4 : 4, v/v/v) as an eluent. In the case of (Et-Cz-BTz)$_2$Ir(EO$_2$-pic) and (Et-Cz-BTz)$_2$Ir(EO$_2$-pic-N-O), the chlorine substituent in 4-chloropicolinic acid and 4-chloropicolinic acid N-oxide was replaced by ethoxyethanol by tandem reaction during the synthesis of Ir(III) complexes.

2.4. Bis[2-(9-ethyl-9*H*-carbazol-3-yl)benzothiazole]iridium picolinic acid (Et-Cz-BTz)$_2$Ir(pic)

Yield: 0.31 g, 56 %, m.p. 331 °C. ^{1}H-NMR (300 MHz, $CDCl_3$): δ (ppm): 8.57 (d, 1H), 8.43 (d, 2H), 8.21 (d, 1H), 8.05–7.97 (m, 2H), 7.88–7.82 (m, 4H), 7.47 (t, 1H), 7.42–7.30 (m, 4H), 7.27–7.08 (m, 5H), 6.94 (t, 1H), 6.51 (s, 1H), 6.21–6.15 (m, 2H), 3.82–3.68 (m, 4H), 0.96 (t, 3H), 0.84 (t, 3H). ^{13}C-NMR ($CDCl_3$): δ (ppm) 182.3, 179.8, 173.3, 153.6, 150.5, 148.9, 147.0, 145.9, 143.3, 143.0, 139.9, 137.9, 133.0, 132.4, 131.7, 131.0, 128.3, 128.0, 126.9, 125.3, 125.2, 125.0, 124.4, 124.0, 123.8, 123.1, 122.1, 121.2, 119.8, 119.5, 119.4, 119.3, 119.2, 118.7, 118.5, 113.1, 112.9, 108.8, 108.5, 100.1, 37.4, 37.2, 13.1, 12; anal. calcd for $C_{48}H_{34}IrN_5O_2S_2$: C, 59.49; H, 3.54; N, 7.23; S, 6.62. Found: C, 59.27; H, 3.49; N, 7.04; S, 6.36. HRESI-MS $[M + H]^+$: m/z calcd for 969.1996, found 969.1964.

2.5. Bis[2-(9-ethyl-9*H*-carbazol-3-yl)benzothiazole]iridium picolinic acid *N*-oxide (Et-Cz-BTz)$_2$Ir(pic-N-O)

Yield: 0.32 g, 57 %, m.p. 325 °C. ^{1}H-NMR (300 MHz, $CDCl_3$): δ (ppm) 8.57 (d, 1H), 8.43 (d, 2H), 8.21 (d, 1H), 8.05–7.97 (m, 2H), 7.89–7.82 (m, 4H), 7.47 (t, 1H), 7.41–7.28 (m, 5H), 7.25–7.09 (m, 4H), 6.94 (t, 1H), 6.51 (s, 1H), 6.22–6.15 (m, 2H), 3.82–3.68 (m, 4H), 0.95 (t, 3H), 0.84 (t, 3H). ^{13}C-NMR ($CDCl_3$): δ (ppm) 182.3, 179.8, 173.3, 153.6, 150.6, 150.5, 148.9, 147.1, 146.0, 143.3, 143.0, 140.0, 137.9, 133.0, 132.5, 131.7, 131.0, 128.3, 128.0, 126.9, 125.3, 125.2, 125.0, 124.4, 123.9, 123.8, 123.1, 122.2, 121.2, 119.8, 119.5, 119.3, 119.2, 118.7, 118.5, 113.1, 112.9, 108.8, 108.5, 37.4, 37.2, 13.1, 12.9; anal. calcd for $C_{48}H_{34}IrN_5O_3S_2$: C, 58.52; H, 3.48; N, 7.11; S, 6.51. Found: C, 58.72; H, 3.48; N, 7.21; S, 6.25. HRESI-MS $[M + H]^+$: m/z calcd for 985.1687, found 985.1643.

2.6. Bis[2-(9-ethyl-9*H*-carbazol-3-yl)benzothiazole]iridium-4-(2-ethoxyethoxy)picolinic acid (Et-Cz-BTz)$_2$Ir(EO$_2$-pic)

Yield: 0.26 g, 43 %, m.p. 282 °C. ^{1}H-NMR (300 MHz, $CDCl_3$): δ (ppm) 8.54–8.38 (m, 3H), 8.04–7.94 (m, 2H), 7.90–7.83 (m, 2H), 7.73–7.70 (m, 1H), 7.60–7.55 (m, 1H), 7.46–7.28 (m, 5H), 7.25–7.08 (m, 3H), 7.06–7.01 (m, 2H), 6.86–6.85 (m, 1H), 6.50 (s, 1H), 6.36 (t, 1H), 6.24 (s, 1H), 4.20–4.17 (m, 2H), 3.80–3.65 (m, 6H), 3.54 (q, 2H), 1.19 (t, 3H), 0.95 (t, 3H), 0.84 (t, 3H). ^{13}C-NMR ($CDCl_3$): δ (ppm) 182.3, 179.6, 173.3, 166.5, 155.3, 150.6, 149.1, 147.4, 146.1, 143.3, 143.0, 139.9, 133.2, 132.5, 131.6, 131.0, 128.2, 127.1, 125.3, 125.1, 124.9, 124.4, 124.0, 123.8, 123.0, 122.2, 121.2, 119.7, 119.5, 119.3, 119.2, 119.1, 118.6, 117.9, 116.4, 113.1, 113.0, 112.5, 108.8, 108.5, 68.5, 68.3, 67.1, 37.4, 37.2, 15.2, 13.1, 12.9; anal. calcd for $C_{52}H_{42}IrN_5O_4S_2$: C, 59.07; H, 4.00; N, 6.62; S, 6.07. Found: C, 58.34; H, 3.99; N, 6.28; S, 5.91. HRESI-MS $[M + H]^+$: m/z calcd for 1057.2754, found 1057.2723.

2.7. Bis[2-(9-ethyl-9*H*-carbazol-3-yl)benzothiazole]iridium-4-(2-ethoxyethoxy)picolinic acid N-oxide (Et-Cz-BTz)$_2$Ir(EO$_2$-pic-N-O)

Yield: 0.30 g, 49 %, m.p 277 °C. ^{1}H-NMR (300 MHz, $CDCl_3$): δ (ppm) 8.52 (d, 1H), 8.43 (d, 2H), 8.04–7.97 (m, 2H), 7.91–7.87 (m, 2H), 7.73 (d, 1H), 7.60 (d, 1H), 7.45 (t, 1H), 7.41–7.28 (m, 4H), 7.20–7.11 (m, 4H), 7.08–7.04 (m, 1H), 6.89–6.86 (m, 1H), 6.50 (s, 1H), 6.38 (d, 1H), 6.23 (s, 1H), 4.21–4.18 (m, 2H), 3.80–3.68 (m, 6H), 3.54 (q, 2H), 1.20 (t, 3H), 0.95 (t, 3H), 0.84 (t, 3H). ^{13}C-NMR ($CDCl_3$): δ (ppm) 182.3, 179.6, 173.3, 166.5, 166.5, 155.3, 150.5, 149.1, 147.4, 146.1, 143.3, 143.1, 139.9, 133.2, 132.5, 131.6, 131.0, 128.2, 127.1, 125.3, 124.9, 124.4, 124.0, 123.8, 123.0, 122.2, 121.2, 119.7, 119.5, 119.3, 119.2, 119.1, 118.6, 117.9, 116.4, 113.1, 113.0, 112.5, 108.8, 108.5, 68.3, 67.1, 15.2, 13.1, 12.9; anal. calcd for $C_{52}H_{42}IrN_5O_5S_2$: C, 58.19; H, 3.94; N, 6.53; S, 5.98. Found: C, 58.36; H, 4.11; N, 6.54; S, 5.81. HRESI-MS $[M + H]^+$: m/z calcd for 1073.2386, found 1073.2372.

2.8. Device fabrication and characterization

A patterned indium tin oxide (ITO) glass substrate (10 Ω sq^{-1}) was UV-ozone treated for 20 min. A high WF GraHIL was spin-cast onto the substrate and immediately baked in air at 150 °C for 30 min, giving a 40 nm thick film. The EML solutions composed of each dopant and TCTA : TPBI (mixed host) (15 : 100 by wt) dissolved in tetrahydrofuran:CF co-solvent (8 : 2 by wt) or tetrahydrofuran solvent were spin coated on top of the GraHIL in a glove box and baked to give the ~40 nm film. Then, TPBI (50 nm), LiF (1 nm), and Al (90 nm) were thermally deposited under high vacuum (<5 × 10^{-7} Torr). The current density–voltage–luminance characteristics were measured using a Keithley 236 power source measurement unit and a Minolta CS-2000 Spectroradiometer.

3. Results and discussion

Solution-processed yellow PhOLEDs have garnered much attention in recent years due to their easy fabrication, cost effectiveness, and large area lighting applications. For this purpose, four Ir(III) complexes, *i.e.* (Et-Cz-BTz)$_2$Ir(pic), (Et-Cz-BTz)$_2$Ir(pic-N-O), (Et-Cz-BTz)$_2$Ir(EO$_2$-pic), and (Et-Cz-BTz)$_2$Ir(EO$_2$-pic-N-O), were synthesized according to the synthetic route, as shown in Scheme 1. The boronic ester derivative of Cz (1) was prepared according to our previous report with quantitative yield. Then, the compound was reacted with 2-bromobenzothiazole in a Suzuki coupling reaction to obtain the desired donor–acceptor 2-(9-ethyl-9*H*-carbazol-3-yl)benzothiazole (Et-Cz-BTz) based ligand in 62% yield.

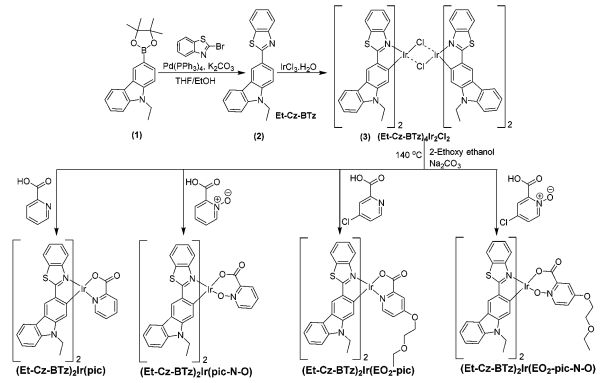

Scheme 1 Synthetic route for (Et-Cz-BTz)$_2$Ir(pic), (Et-Cz-BTz)$_2$-Ir(pic-N-O), (Et-Cz-BTz)$_2$Ir(EO$_2$-pic), and (Et-Cz-BTz)$_2$Ir(EO$_2$-pic-N-O).

The resultant Et-Cz-BTz was reacted with iridium trichloride hydrate ($IrCl_3 \cdot H_2O$) to obtain the cyclometalated Ir(III) μ-chloride bridged dimer $[(\text{Et-Cz-BTz})_4Ir_2Cl_2]$ in quantitative yield. This can be easily converted to the heteroleptic Ir(III) complexes, $(\text{Et-Cz-BTz})_2Ir(pic)$, $(\text{Et-Cz-BTz})_2Ir(pic\text{-}N\text{-}O)$, $(\text{Et-Cz-BTz})_2Ir(EO_2\text{-}pic)$, and $(\text{Et-Cz-BTz})_2Ir(EO_2\text{-}pic\text{-}N\text{-}O)$, by replacing two bridge chlorides with bidentate monoanionic ancillary ligands such as picolinic acid (pic), picolinic acid N-oxide (pic-N-O), 4-chloropicolinic acid, and 4-chloropicolinic acid N-oxide, respectively, with good yield. To enhance the solubility of the Ir(III) complexes, the ethoxyethanol group was introduced into $(\text{Et-Cz-BTz})_2Ir(EO_2\text{-}pic)$ and $(\text{Et-Cz-BTz})_2Ir(EO_2\text{-}pic\text{-}N\text{-}O)$ through a tandem reaction, which was applied to Ir(III) complexes in our previous report for the first time.[13] This can reduce the synthetic steps with good yield. Here, the reaction of 4-chloropicolinic acid or 4-chloropicolinic acid N-oxide and cyclometalated Ir(III) μ-chloride bridged dimer, and the replacement of chlorine in 4-chloropicolinic acid or 4-chloropicolinic acid N-oxide by the ethoxyethanol group, occurred simultaneously in one step. All the Ir(III) complexes are readily soluble in common organic solvents such as methylene chloride (MC), chloroform (CF), and ethyl acetate (EA). The chemical structures of the Ir(III) complexes were confirmed by the ^{1}H-NMR, ^{13}C-NMR and HR-ESI mass spectral techniques.

The thermal stabilities of the Ir(III) complexes were determined by thermogravimetric analysis (TGA) and differential scanning calorimeter (DSC) analysis under N_2 atmosphere at a heating rate of 10 °C min^{-1}, and the corresponding TGA thermograms are shown in Fig. 1. The thermal decomposition temperatures (T_d) at 5% weight loss of $(\text{Et-Cz-BTz})_2Ir(pic)$, $(\text{Et-Cz-BTz})_2Ir(pic\text{-}N\text{-}O)$, $(\text{Et-Cz-BTz})_2Ir(EO_2\text{-}pic)$, and $(\text{Et-Cz-BTz})_2Ir(EO_2\text{-}pic\text{-}N\text{-}O)$ were 403, 394, 356, and 349 °C, respectively, revealing their high thermal stability, which is more favourable for the long term stability of OLEDs.

Among the Ir(III) complexes, the pic-containing Ir(III) complexes show greater thermal stability than the pic-N-O ancillary ligand. On the one hand, the ethoxyethanol solubilizing group linked Ir(III) complexes, $(\text{Et-Cz-BTz})_2Ir(EO_2\text{-}pic)$ and $(\text{Et-Cz-BTz})_2Ir(EO_2\text{-}pic\text{-}N\text{-}O)$, show lower T_d values than their counterparts, but, the ethoxyethanol group increases the solubility of the Ir(III) complexes, which aids in the fabrication of PhOLEDs using solution-processed techniques. The DSC thermograms of all Ir(III) complexes show the glass transition temperatures (T_g), which were in the range of 161–247 °C without any crystalline and melting peaks. This suggests that all synthesized Ir(III) complexes will not easily distort under high temperatures that are produced during the operation of PhOLEDs.

The photophysical properties of the main ligand, (Et-Cz-BTz), and the Ir(III) complexes, $(\text{Et-Cz-BTz})_2Ir(pic)$, $(\text{Et-Cz-BTz})_2Ir(pic\text{-}N\text{-}O)$, $(\text{Et-Cz-BTz})_2Ir(EO_2\text{-}pic)$, and $(\text{Et-Cz-BTz})_2Ir(EO_2\text{-}pic\text{-}N\text{-}O)$, were measured using UV-visible absorption and photoluminescence (PL) spectra at room temperature in the CF solution. Fig. 2a shows the UV-visible absorption spectra of the main ligand, (Et-Cz-BTz), and the Ir(III) complexes in the CF solution. Et-Cz-BTz shows intense absorption between 320 and 375 nm with a peak at 345 nm, attributed to the spin-allowed $^1\pi$–π^* transitions of the Cz and BTz moieties. All the Ir(III) complexes show three absorption maxima in three different regions, as shown in Fig. 2a. The absorption bands in the higher energy region below 360 nm

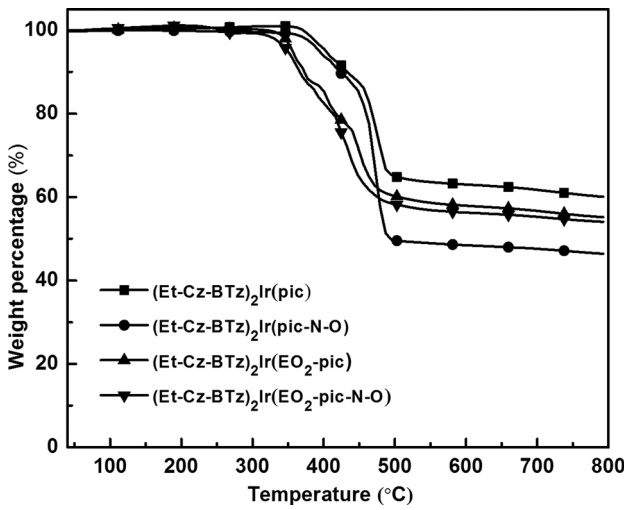

Fig. 1 TGA of $(\text{Et-Cz-BTz})_2Ir(pic)$, $(\text{Et-Cz-BTz})_2Ir(pic\text{-}N\text{-}O)$, $(\text{Et-Cz-BTz})_2Ir(EO_2\text{-}pic)$ and $(\text{Et-Cz-BTz})_2Ir(EO_2\text{-}pic\text{-}N\text{-}O)$ measured at a scan rate of 10 °C min^{-1} under a N_2 atmosphere.

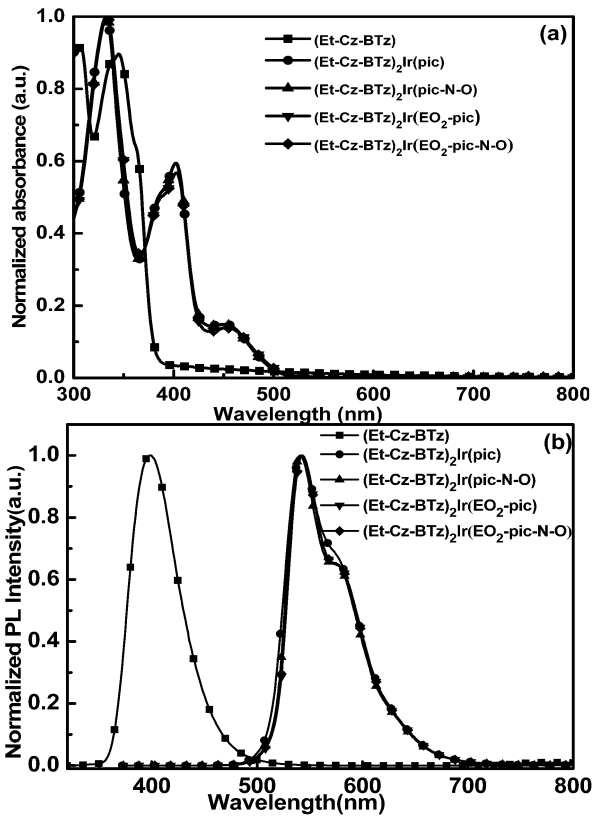

Fig. 2 (a) UV-visible absorption and (b) PL spectra of $(\text{Et-Cz-BTz})_2Ir(pic)$, $(\text{Et-Cz-BTz})_2Ir(pic\text{-}N\text{-}O)$, $(\text{Et-Cz-BTz})_2Ir(EO_2\text{-}pic)$, and $(\text{Et-Cz-BTz})_2Ir(EO_2\text{-}pic\text{-}N\text{-}O)$ in chloroform at 25 °C.

correspond to the spin-allowed $^1\pi$–π^* transitions of the cyclometalated ligands, which closely resembles the absorption spectrum of the main ligand. The weak absorption bands between 370 and 500 nm are likely due to metal-to-ligand charge-transitions (^{1}MLCT and ^{3}MLCT) and the spin-orbit coupling enhanced $^3\pi$–π^* states. The absorption pattern of all Ir(III) complexes are almost identical to each other, indicating that the introduction of the ethoxyethanol group on the 4-position of the ancillary ligands does not greatly affect the absorption spectra.

The PL spectra of the ligand and the Ir(III) complexes in the CF solution are shown in Fig. 2b. All the Ir(III) complexes show very similar PL patterns with a maximum at 541 nm and a shoulder at 582 nm, irrespective of the nature of the substituent on the ancillary ligand. This indicates that the presence of an ethoxyethanol solubilizing group in ancillary ligands will increase only the solubility of the Ir(III) complexes rather than any of the photophysical properties. When compared to the PL maxima of Tz-based Ir(III) complexes,[13] the BTz-based Ir(III) complexes show only a 5 nm red shift in the maxima in the CF solution. Under photoexcitation at their absorption maximum, all Ir(III) complexes emit yellow light in the PL spectra (Fig. 2b). In comparison to Et-Cz-BTz, which emits deep blue fluorescence at 398 nm, all the Ir(III) complexes display a strongly red shifted PL band (λ_{em}: ~541–543 nm) at room temperature upon excitation at 386 nm, which is associated predominantly with a ligand-centred $^3\pi$–π^* excited state.

To investigate the charge carrier injection properties of the Ir(III) complexes, the highest occupied molecular orbital (HOMO) and lowest unoccupied molecular orbital (LUMO) were determined using cyclic voltammetry (CV). The cyclic voltammograms of all the Ir(III) complexes are shown in Fig. 3. All Ir(III) complexes display reversible redox waves over both the anodic and cathodic ranges, suggesting that the stable Ir(II) and Ir(IV) radicals are formed from the Ir(III) complexes (Table 1).

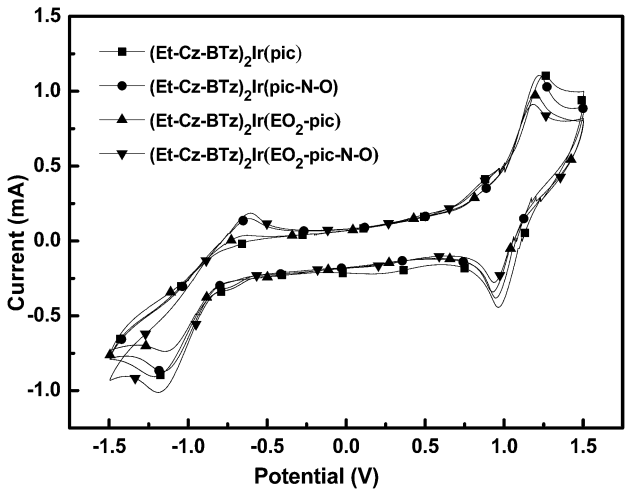

Fig. 3 Cyclic voltammograms of (Et-Cz-BTz)$_2$Ir(pic), (Et-Cz-BTz)$_2$Ir(pic-N-O), (Et-Cz-BTz)$_2$Ir(EO$_2$-pic), and (Et-Cz-BTz)$_2$Ir(EO$_2$-pic-N-O) in tetra-butylammoniumtetrafluoroborate (TBABF$_4$) at a scan rate of 100 mV s^{-1}.

The onset oxidation potentials were in the range of 1.00–1.02 eV and the corresponding HOMO energy levels were found to be −5.24 to −5.26 eV with ferrocene/ferrocenium as a reference redox system (4.8 eV under vacuum). The band gaps were calculated using the UV-visible absorption edge and were in the range of ~2.45 eV, which is within the error limits (0.1–0.7 eV) of E_g^{opt}, and the corresponding LUMO energy levels were found to be −2.75 to −2.81 eV.

We fabricated yellow emitting solution-processed PhOLEDs with the device structure shown in Fig. 4a. It is very important to realize efficient solution-processed PhOLEDs with a simple structure, and efficient blocking of electrons and quenching of excitons to increase the radiative decay as well as the efficient hole injection to the EML at the HIL/EML interface.[27]

We exploited a self-organized polymeric HIL that is composed of a conventional conducting polymer, poly(3,4-ethylenedioxythiphene):poly(styrene sulfonate) (PEDOT:PSS), and a perfluorinated polymeric acid with a low surface energy, tetrafluoroethylene-perfluoro-3,6-dioxa-4-methyl-7-octene- sulfonic acid copolymer (PFI), in 1 : 1 weight ratio (GraHIL).[27–31] These polymers develop a gradient WF, which gradually increases from the bottom surface (~4.8 eV) to the top surface (~5.95 eV) due to self-organization of PFI. It then facilitates hole injection and transport to the EML by reducing the hole injection barrier between the WF of the HIL and the HOMO energy level of the EML. The large quantity of the insulating PFI on the HIL surface also blocks electron injection and blocks quenching of excitons. Thus, the PhOLEDs with GraHIL do not require any overlying hole transport layer (HTL) or electron blocking layer (EBL).

We fabricated the EML by spin coating a solution of yellow emitting phosphorescence dopant, a mixed host system consisting of a hole transporting host, 4,4′,4″-tris(*N*-carbazolyl)triphenylamine (TCTA), and an electron transporting host, 1,3,5-tris(*N*-phenylbenzimidizol-2-yl)benzene (TPBI), in 1 : 1 weight ratio using tetrahydrofuran:CF (8 : 2) co-solvent on top of the GraHIL (Fig. 4a). The solution-processed PhOLEDs were fabricated with the configuration of ITO/GraHIL (40 nm)/TCTA:TPBI:Ir(III) complexes (15 wt%) (40 nm)/TPBI (50 nm)/LiF (1 nm)/Al (90 nm). The bipolar characteristics of the mixed host are advantageous to improve device efficiency by broadening the recombination zone (Table 2).[32]

The current density–voltage and luminance-voltage curves of PhOLEDs with 4 different dopants are given in Fig. 4b and c, respectively. The maximum current efficiencies (CE) and EQE of PhOLEDs with [(Et-Cz-BTz)$_2$Ir(pic)], [(Et-Cz-BTz)$_2$Ir(pic-N-O)], [(Et-Cz-BTz)$_2$Ir(EO$_2$-pic)], and [(Et-Cz-BTz)$_2$Ir(EO$_2$-pic-N-O)] were found to be (40 cd A^{-1}, 12.5%), (32.5 cd A^{-1}, 10%), (52 cd A^{-1}, 16.5%), and (50 cd A^{-1}, 15.5%), respectively (Fig. 4d and e). PhOLEDs with 4 different dopants showed the same yellow spectrum with a maximum electroluminescence (EL) peak at ~550 nm and shoulder at ~590 nm, which correspond well with the PL spectra (Fig. 2b) at 1000 cd m^{-2} (Fig. 4f). One of the major observations in solution processed PhOLEDs is the morphology; hence, the morphology of the EML determines the efficiency of the device performance. We also measured the surface roughness of neat TCTA : TPBI film and TCTA : TPBI

Table 1 Photophysical, electrochemical and thermal properties of Ir(III) complexes

Compound	T_d[a] [°C]	T_g[b] [°C]	λ_{em}[c] [nm]	Φ_{pl}[d]	HOMO/LUMO[e] [eV]
(Et-Cz-BTz)$_2$Ir(pic)	403	161	541, 578	0.10	−5.26/−2.75
(Et-Cz-BTz)$_2$Ir (pic-N-O)	394	247	541, 582	0.11	−5.26/−2.81
(Et-Cz-BTz)$_2$Ir (EO$_2$-pic)	356	233	543, 582	0.12	−5.24/−2.79
(Et-Cz-BTz)$_2$Ir (EO$_2$-pic-N-O)	349	241	542, 582	0.11	−5.26/−2.80

[a] Temperature with 5% mass loss measured by TGA with a heating rate of 10 °C min^{-1} under N_2. [b] Glass transition temperature, determined by DSC with a heating rate of 10 °C min^{-1} under N_2. [c] Maximum emission wavelength, measured in CF solution at 1.0×10^{-5} M. [d] Measured in 1×10^{-5} M $CHCl_3$ solution relative to Ir(piq)$_2$(acac) (Φ_{pl} = 0.20) with 455 nm excitation. [e] Determined from the onset of CV for oxidation and UV-visible absorption edge.

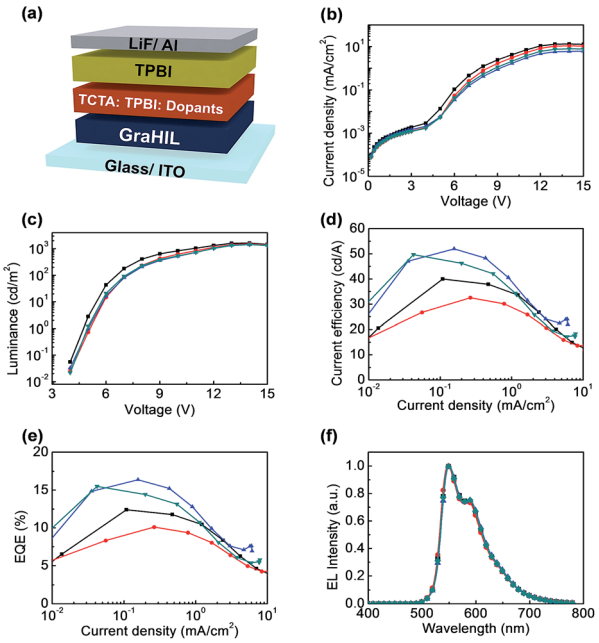

Fig. 4 (a) Device structure of yellow emitting PhOLEDs fabricated by spin coating the EML dissolved in tetrahydrofuran:CF co-solvent; (b) current density–voltage curves of PhOLEDs with various yellow-emitting dopants ((—■—) [(Et-Cz-BTz)$_2$Ir(pic)], (—●—) [(Et-Cz-BTz)$_2$Ir(pic-N-O)], (—▲—) [(Et-Cz-BTz)$_2$Ir(EO$_2$-pic)] and (—▼—) [(Et-Cz-BTz)$_2$Ir(EO$_2$-pic-N-O)]); (c) luminance-voltage, (d) current efficiency–current density, (e) external quantum efficiency–current density, and (f) EL spectra.

with [(Et-Cz-BTz)$_2$Ir(pic)], [(Et-Cz-BTz)$_2$Ir(pic-N-O)], [(Et-Cz-BTz)$_2$-Ir(EO$_2$-pic)], and [(Et-Cz-BTz)$_2$Ir(EO$_2$-pic-N-O)] and these results are shown in Fig. 5. The root-mean-square (RMS) roughness values of neat TCTA : TPBI film (Fig. 5a) and TCTA : TPBI with [(Et-Cz-BTz)$_2$Ir(pic)] (Fig. 5b), [(Et-Cz-BTz)$_2$Ir(pic-N-O)] (Fig. 5c), [(Et-Cz-BTz)$_2$Ir(EO$_2$-pic)] (Fig. 5d), and [(Et-Cz-BTz)$_2$Ir(EO$_2$-pic-N-O)] (Fig. 5e) were found to be 0.247 nm, 0.231 nm, 0.244 nm, 0.231 nm, and 0.242 nm, respectively. These values indicate that the EMLs have a smooth surface, which reduces the leakage current in the device and induces high luminous efficiency.

We further optimized the solution-processed PhOLEDs, fabricating the EMLs by spin coating the solution dissolved only in THF, and then finally achieved higher device efficiencies (CE: 60 cd A^{-1}, EQE: 19%) (Fig. 6a and b). The EL spectrum of the optimized device was identical to the PL spectrum (Fig. 6c). To the best of our knowledge, these values are the best efficiencies for yellow EML solution-processed PhOLEDs using heteroleptic Ir(III) complexes reported so far. These high efficiencies can be attributed to the good organic solubility of dopants arising from benzothiazole linked ethylcarbazole in Ir(III) complexes and

Table 2 Performances of solution-processed OLEDs with four different yellow emitting Ir(III) complexes

Compound	Solvent	CE_{max} (cd A^{-1})	EQE_{max} (%)
(Et-Cz-BTz)$_2$Ir(pic)	THF : CF (8 : 2)	40	12.5
(Et-Cz-BTz)$_2$Ir(pic-N-O)	THF : CF (8 : 2)	32.5	10
(Et-Cz-BTz)$_2$Ir(EO$_2$-pic)	THF : CF (8 : 2)	52	16.5
(Et-Cz-BTz)$_2$Ir(EO$_2$-pic-N-O)	THF : CF (8 : 2)	50	15.5
(Et-Cz-BTz)$_2$Ir(EO$_2$-pic)	THF	60	19

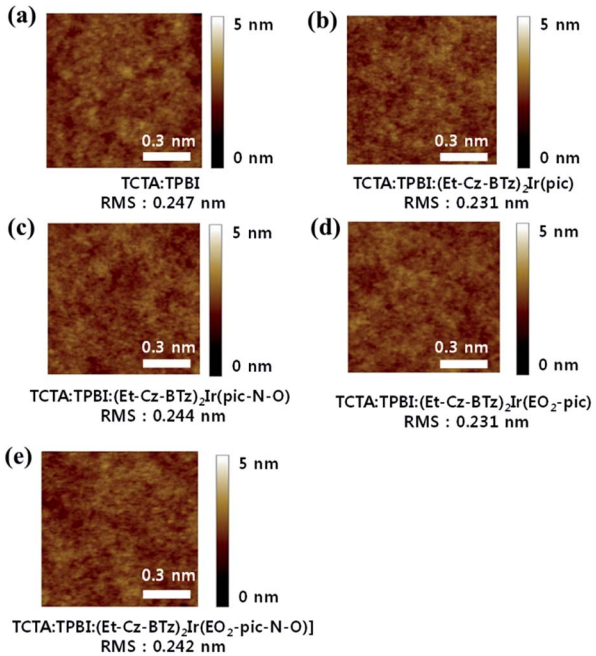

Fig. 5 Atomic force microscopy (AFM) images of (a) TCTA:TPBI, (b) TCTA:TPBI:(Et-Cz-BTz)$_2$Ir(pic), (c) TCTA:TPBI:(Et-Cz-BTz)$_2$Ir(pic-N-O), (d)TCTA:TPBI:(Et-Cz-BTz)$_2$Ir(EO$_2$-pic) and (e) TCTA:TPBI:(Et-Cz-BTz)$_2$-Ir(EO$_2$-pic-N-O).

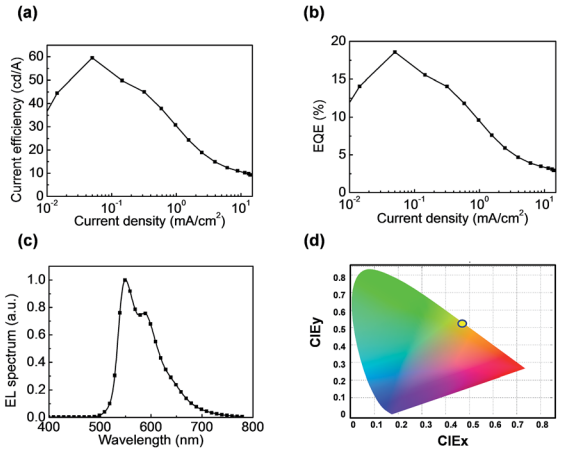

Fig. 6 (a) Current efficiency–current density of yellow-emitting PhOLEDs with (Et-Cz-BTz)$_2$Ir(EO$_2$-pic) fabricated by spin coating the EML dissolved in tetrahydrofuran solvent, (b) external quantum efficiency–current density, (c) EL spectrum and (d) CIE coordinates.

good electron–hole balance in the EML. The Commision Internationale de l'Éclairage (CIE) coordinates of the device are (0.466, 0.525) at 1000 cd m^{-2}, which corresponds well with the yellow region in the CIE chromaticity diagram (Fig. 6d).

4. Conclusions

In summary, we have successfully synthesized four BTz linked Et-Cz based Ir(III) complexes, [(Et-Cz-BTz)$_2$Ir(pic)], [(Et-Cz-BTz)$_2$Ir(pic-N-O)], [(Et-Cz-BTz)$_2$Ir(EO$_2$-pic)], and [(Et-Cz-BTz)$_2$Ir(EO$_2$-pic-N-O)], for solution-processed yellow PhOLEDs, and fabricated devices with the configuration of ITO/GraHIL (40 nm)/TCTA:TPBI:Ir(III) complex (15 wt%) (40 nm)/TPBI (50 nm)/LiF (1 nm)/Al (90 nm). Both Tz and BTz based Ir(III) complexes emit the same bright yellow phosphorescence at room temperature, which indicates that the introduction of BTz into the Et-Cz main ligand instead of Tz does not show a significant effect on the phosphorescence emission of the Ir(III) complexes.[13] Among the four Ir(III) complexes, the most promising Ir(III) complex [(Et-Cz-BTz)$_2$Ir(EO$_2$-pic)] showed the best luminous efficiency of 60 cd A^{-1} and EQE of 19% with CIE coordinates (0.467, 0.524), which is more than three times higher than that of the most promising Ir(III) complex of the Tz counterparts.[13] To the best of our knowledge, this is one of the best solution-processed EML yellow PhOLEDs reported so far. This phenomenon paves an effective way towards improving the efficiency of particular PhOLEDs without changing the color by small modifications in the structure of the main ligands of Ir(III) complexes.

Acknowledgements

This work was supported by grant fund from the National Research Foundation (NRF) (2011-0028320), and the Pioneer Research Center Program through the NRF (NRF-2013M3C1A3065522) and (NRF-2013R1A2A2A01068753) by the Ministry of Science, ICT & Future Planning (MSIP) of Korea.

Notes and references

1 M. A. Baldo, D. F. O'Brien, Y. You, A. Shoustikov, S. Sibley, M. E. Thompson and S. R. Forrest, *Nature*, 1998, **395**, 151–154.
2 Y. Sun, N. C. Giebink, H. Kanno, B. Ma, M. E. Thompson and S. R. Forrest, *Nature*, 2006, **440**, 908–912.
3 B. W. D'Andrade and S. R. Forrest, *Adv. Mater.*, 2004, **16**, 1585–1595.
4 B. D'Andrade, *Nat. Photonics*, 2007, **1**, 33–34.
5 A. Chihaya, M. A. Marc, S. R. Forrest and M. E. Thompson, *Appl. Phys. Lett.*, 2000, **77**, 904–906.
6 E. Holder, B. M. W. Langeveld and U. S. Schubert, *Adv. Mater.*, 2005, **17**, 1109–1121.
7 P. T. Chou and Y. Chi, *Chem. Soc. Rev.*, 2007, **36**, 1421–1431.
8 P. L. Burn, S.-C. Lo and I. D. W. Samuel, *Adv. Mater.*, 2007, **19**, 1675–1688.
9 R. Xiaofan, M. E. Kondakova, D. J. Giesen, M. Rajeswaran, M. Madaras and W. C. Lenhart, *Inorg. Chem.*, 2010, **49**, 1301–1303.
10 M. Tavasli, T. N. Moore, Y. Zheng, M. R. Bryce, M. A. Fox, G. C. Griffiths, V. Jankus, H. A. Al-Attarc and A. P. Monkmanc, *J. Mater. Chem.*, 2012, **22**, 6419–6428.
11 D. Liu, H. Ren, L. Deng and T. Zhang, *ACS Appl. Mater. Interfaces*, 2013, **5**, 4937–4944.
12 J. Li, R. Wang, R. Yang, W. Zhou and X. Wang, *J. Mater. Chem. C*, 2013, **1**, 4171–4179.
13 T. Giridhar, W. Cho, J. Park, J.-S. Park, Y.-S. Gal, S. Kang, J. Y. Lee and S.-H. Jin, *J. Mater. Chem. C*, 2013, **1**, 2368–2378.
14 I. R. Laskar and T. M. Chen, *Chem. Mater.*, 2004, **16**, 111–117.
15 R. J. Wang, D. Liu, R. Zhang, L. J. Deng and J. Y. Li, *J. Mater. Chem.*, 2012, **22**, 1411–1417.
16 R. J. Wang, D. Liu, H. C. Ren, T. Zhang, H. M. Yin, G. Y. Liu and J. Y. Li, *Adv. Mater.*, 2011, **23**, 2823–2827.
17 S. Feng, L. Duan, L. Hou, J. Qiao, D. Zhang, G. Dong, L. Wang and Y. Qiu, *J. Phys. Chem. C*, 2011, **115**, 14278–14284.
18 H. Wu, L. Ying, W. Yang and Y. Cao, *Chem. Soc. Rev.*, 2009, **38**, 3391–3400.
19 G. Zhou, W.-Y. Wong and S. Suo, *J. Photochem. Photobiol., C*, 2010, **11**, 133–156.
20 X.-H. Yang, F.-I. Wu, D. Neher, C.-H. Chien and C.-F. Shu, *Chem. Mater.*, 2008, **20**, 1629–1635.
21 Z. Ma, J. Ding, B. Zhang, C. Mei, Y. Cheng, Z. Xie, L. Wang, X. Jing and F. Wang, *Adv. Funct. Mater.*, 2010, **20**, 138–146.
22 S. Gambino, S.-C. Lo, Z. Liu, P. L. Burn and I. D. W. Samuel, *Adv. Funct. Mater.*, 2012, **22**, 157–165.
23 J. W. Levell, S. Zhang, W.-Y. Lai, S.-C. Lo, P. L. Burn and I. D. W. Samuel, *Opt. Express*, 2012, **20**, A213–A218.
24 S. J. Lee, J. S. Park, M. Song, I. A. Shin, Y. I. Kim and S.-H. Jin, *Adv. Funct. Mater.*, 2009, **19**, 2205–2212.
25 M. Song, J. S. Park, Y. S. Gal, S. Kang, J. Y. Lee, J. W. Lee and S.-H. Jin, *J. Phys. Chem. C*, 2012, **116**, 7526–7533.

26 M. Song, J. S. Park, M. Yoon, A. J. Kim, Y. I. Kim, Y. S. Gal, S. Kang, J. Y. Lee, J. W. Lee and S.-H. Jin, *J. Organomet. Chem.*, 2011, **696**, 2122–2128.
27 T. H. Han, M.-R. Choi, S.-H. Woo, S.-Y. Min, C.-L. Lee and T.-W. Lee, *Adv. Mater.*, 2012, **24**, 1487–1493.
28 T.-W. Lee, Y. Chung, O. Kwon and J.-J. Park, *Adv. Funct. Mater.*, 2007, **17**, 390–396.
29 T.-H. Han, Y. Lee, M.-R. Choi, S.-H. Woo, S.-H. Bae, B. H. Hong, J.-H. Ahn and T.-W. Lee, *Nat. Photonics*, 2012, **6**, 105–110.
30 M.-R. Choi, T.-H. Han, K.-G. Lim, S.-H. Woo, D. H. Huh and T.-W. Lee, *Angew. Chem., Int. Ed.*, 2011, **50**, 6274–6277.
31 M.-R. Choi, S.-H. Woo, T.-H. Han, K.-G. Lim, S.-Y. Min, W. M. Yun, O. K. Kwon, C. E. Park, K.-D. Kim, H.-K. Shin, M.-S. Kim, T. Noh, J. H. Park, K.-H. Shin, J. Jang and T.-W. Lee, *ChemSusChem*, 2011, **4**, 363–368.
32 M. E. Kondakova, T. D. Pawlik, R. H. Young, D. J. Giesen, D. Y. Kondakov, C. T. Brown, J. C. Deaton, J. R. Lenhard and K. P. Klubek, *J. Appl. Phys.*, 2008, **104**, 094501–094517.